Available online at www.sciencedirect.com
SCIENCE DIRECT
Journal of Power Sources 156 (2006) 306–310
JOURNAL OF POWER SOURCES
www.elsevier.com/locate/jpowsour

Short communication

Anode-supported SOFC with 1Ce10ScZr modified cathode/electrolyte interface

Zhenwei Wang [a,b], Mojie Cheng [a,*], Yonglai Dong [a], Min Zhang [a,b], Huamin Zhang [a]

[a] *Dalian Institute of Chemical Physics, The Chinese Academy of Sciences, Dalian 116023, PR China*
[b] *Graduate School of Chinese Academy of Sciences, Beijing 100039, PR China*

Received 21 March 2005; received in revised form 15 June 2005; accepted 27 June 2005
Available online 6 September 2005

Abstract

The cathode/electrolyte interface in anode-supported solid oxide fuel cells (SOFCs) with Ni–8 mol% yttria-stabilized zirconia (YSZ) anode, thin YSZ electrolyte and $La_{0.8}Sr_{0.2}Mn_{1.1}O_{3-\delta}$ (LSM)–YSZ composite cathode was modified by dispersed $(CeO_2)_{0.01}$–$(Sc_2O_3)_{0.10}$–$(ZrO_2)_{0.89}$ (1Ce10ScZr) electrolyte. The two electrolytes were co-fired into a dense and continuous electrolyte film. By this method, the electrode polarization resistance, specifically the charge transfer resistance of oxygen ions, was greatly reduced. The modified cell achieved a higher performance than the unmodified one, especially at the lower operation temperatures. The decrease of electrode polarization resistance can be ascribed to the accelerated surface oxygen exchange rate from 1Ce10ScZr electrolyte at the cathode/electrolyte interface.

Keywords: Anode-supported SOFC; Cathode/electrolyte interface; 1Ce10ScZr; Surface oxygen exchange

1. Introduction

Solid oxide fuel cell (SOFC) provides a highly efficient and environmentally friendly power generation system. In recent years, enormous research efforts are orientated to the intermediate-temperature SOFC (IT-SOFC, operated at 650–800 °C) [1–5] in order to meet various application requirements. Among various cell structures, the anode-supported SOFC with a thin YSZ electrolyte and an LSM–YSZ composite cathode achieves a leading development [6–9]. In the intermediate-temperature range, however, the cathode overpotential grows significantly and becomes the main issue affecting the cell performance [6,8,9].

Some highly active cathode materials, such as $La_{0.6}Sr_{0.4}CoO_{3-\delta}$ (LSC) [5,10] and $La_{0.8}Sr_{0.2}FeO_{3-\delta}$ (LSF) [11], are applied as alternatives of the LSM–YSZ composite cathode. A buffer layer of a doped ceria electrolyte is usually required to avoid the deleterious reactions [5,10–12]. Unfortunately, solid-state reactions can also occur between the ceria interlayer and the YSZ electrolyte during co-firing at above 1300 °C [13,14]. On the other hand, a doped ceria electrolyte shows a different thermal expansion coefficient from the YSZ electrolyte, and it is fragile against various mechanical stresses. Therefore, the LSM–YSZ composite cathode is still the preferential choice for the YSZ electrolyte until now.

The cathode/electrolyte interface is also an important origin of internal efficiency loss for anode-supported SOFC [6,15–19]. To optimize the interface, introducing a thin interlayer with higher oxygen ionic conductivity, such as a doped ceria electrolyte, could greatly reduce the electrode impedance [20–22]. On the other hand, besides adopting the LSM–YSZ composite cathode, the three-phase-boundary length (TPBL) for oxygen reduction can be extended through sintering individual YSZ particles on a thick YSZ membrane for pure LSM cathode [23,24].

Compared with the YSZ electrolyte, the $(CeO_2)_{0.01}$–$(Sc_2O_3)_{0.10}$–$(ZrO_2)_{0.89}$ (1Ce10ScZr) electrolyte displays much higher oxygen ionic conductivity [25,26] and the two

* Corresponding author. Tel.: +86 411 84379049; fax: +86 411 84379049.
E-mail address: mjcheng@dicp.ac.cn (M. Cheng).

0378-7753/$ – see front matter © 2005 Elsevier B.V. All rights reserved.
doi:10.1016/j.jpowsour.2005.06.035

electrolytes show good chemical compatibility and similar thermal expansion coefficients. In this paper, the 1Ce10ScZr electrolyte particles were implanted onto the surface of YSZ thin film to optimize the cathode/electrolyte interface. The structure and electrochemical performance of the anode-supported SOFC were investigated.

2. Experimental

Sc_2O_3 was supplied from Rare-Chem Hi-Tech Corporation of China. $(CeO_2)_{0.01}$–$(Sc_2O_3)_{0.10}$–$(ZrO_2)_{0.89}$ electrolyte powder, with an average particle size of about 0.5 μm, was prepared by the co-precipitating method, and calcined at 600 °C for 2 h. $La_{0.8}Sr_{0.2}Mn_{1.1}O_{3-\delta}$ (LSM) was synthesized through a combined citrate and EDTA complexing method, and calcined at 1100 °C for 2 h to get a pure perovskite phase. The 8 mol% yttria-stabilized zirconia (YSZ, Tosoh Corporation, Japan) and nickel oxide (NiO, J.T. Baker Corporation, American) were used without further purification.

YSZ thin film supported on NiO–YSZ (50:50, wt.%) substrate was fabricated by the tape-casting method with suitable organic binders, and then made into green bodies of 25 mm diameter. The 1Ce10ScZr particles were dry-coated directly onto the green YSZ film surface, in which the particles were spread on the surface through wiping with a soft plastic film. At last, about 0.2 mg cm^{-2} of 1Ce10ScZr electrolyte was left on the YSZ surface. After pressed under 94 MPa, the green assembly was co-fired at 1400 °C for 2 h. The anode substrate and the densed YSZ electrolyte layer were 700 and 15 μm in thickness, respectively. The LSM–YSZ (50:50, wt.%) composite cathode was applied onto the electrolyte film by the screen-printing method, and fired at 1200 °C for 2 h. The cathode was about 0.50 cm^2 in area and about 50 μm in thickness.

To test cell performance, H_2 mixed with water vapor (3 vol.%) and pure O_2 were fed into the anode and the cathode at a flow rate of 100 ml min^{-1}, respectively. The two-probe electrochemical impedance spectra (EIS) were measured in the frequency range of 50 kHz to 0.1 Hz with the amplitude of 10 mV under open circuit condition.

The electrolyte surface morphology was examined by optical microscopy (OM, Keyence-VK8510) before firing. The modified cell was also observed by scanning electron microscopy (XL-30) after cell test.

3. Results and discussion

3.1. Structure of electrolyte layer

Fig. 1 gives the OM graphs of the green electrolyte film surfaces with and without 1Ce10ScZr modification. The unmodified YSZ film exhibits a smooth surface (Fig. 1a). After the dry coating of 1Ce10ScZr, the YSZ film surface is partially covered with some white 1Ce10ScZr particles (Fig. 1b), which are tightly combined with the YSZ layer after

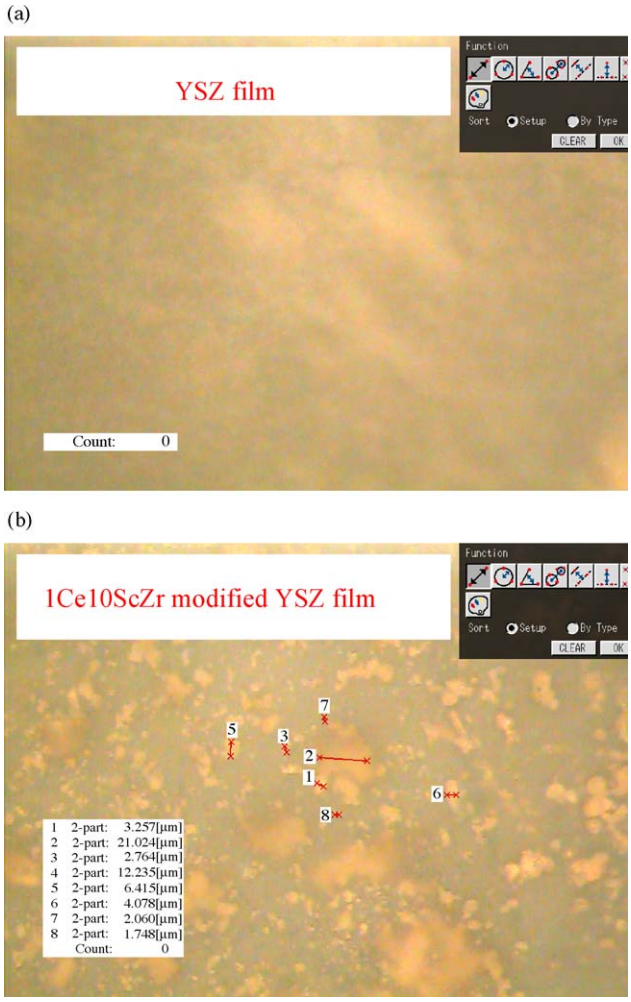

Fig. 1. Optical micrographs of the green electrolyte film surface: (a) before modification and (b) after 1Ce10ScZr modification.

pressed. Fig. 2 displays the SEM micrograph of the cross-section of the modified cell. The electrolyte film is dense and continuous without any pinholes or cracks. Owing to the good chemical compatibility and the similar thermal expansion coefficients, the two electrolytes are sintered together very well. As a result, it is difficult to discriminate 1Ce10ScZr grains at cathode/electrolyte interface from the YSZ electrolyte layer. This is different from the obvious interface between ceria buffer layer (or interlayer) and YSZ thin film by a two-step sintering process [11]. The modification of cathode/electrolyte interface with 1Ce10ScZr does not destroy the structure of the YSZ electrolyte layer, and a good gas tightness characteristic is kept.

3.2. EIS analysis

Fig. 3 displays the EIS spectra of the cells measured at 650 °C under open circuit conditions. The high frequency arc, ranging from 50 kHz to 50 Hz, is obviously suppressed after the 1Ce10ScZr modification. The arc in this frequency range depends mainly on the charge transfer processes of

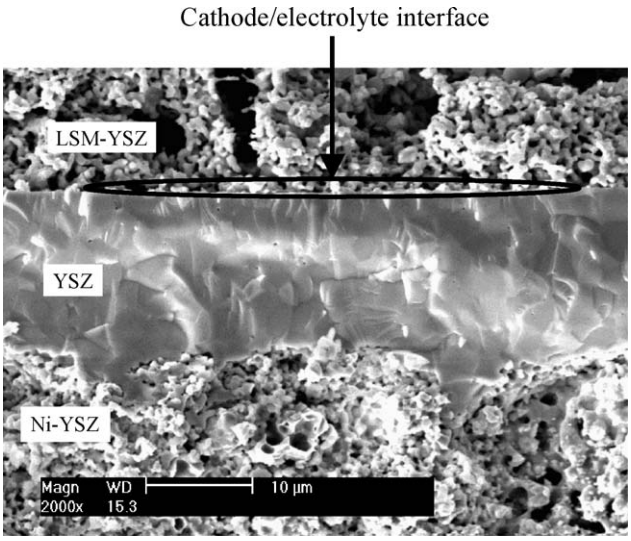

Fig. 2. SEM graph of the cross-section of the 1Ce10ScZr modified cell.

oxide ions from the LSM–YSZ composite cathode to the YSZ electrolyte [9]. Generally speaking, the exchange current density at the cathode/electrolyte interface is in proportion to the ionic conductivity of the applied electrolyte [25]. The oxygen ionic conductivity of scandia-stabilized zirconia electrolyte is about two to three times of that of YSZ in the intermediate-temperature range [26,27]. Therefore, the 1Ce10ScZr modification on YSZ film surface promotes the charge transfer processes. Another possible reason may be related to the small quantity of CeO_2 in the 1Ce10ScZr electrolyte. Steel reported that doping with larger redox cation can enhance the injection of oxide ions into solid electrolyte [28]. Especially, the Ce^{4+}/Ce^{3+} redox reaction is favored at surface sites. So, CeO_2 in 1Ce10ScZr electrolyte may also improve the surface oxygen exchange rate of electrolyte layer.

Fig. 3 also shows the similar ohmic resistances between the modified cell and the unmodified one. It can be deduced

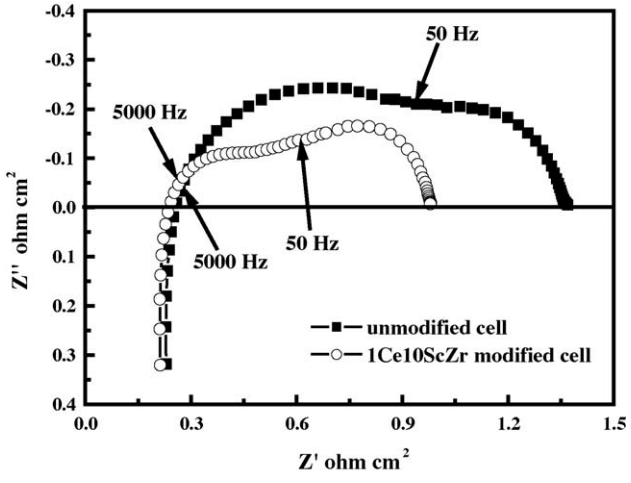

Fig. 3. Electrochemical impedance spectra of the single cells with and without the 1Ce10ScZr modification. The spectra were measured at 650 °C and under open circuit conditions.

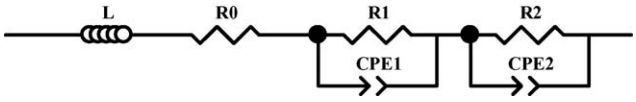

Fig. 4. Electrochemical impedance model. L, inductor; R_0, ohmic resistance; R_1, resistance of high frequency arc; CPE1, constant phase element of high frequency arc; R_2, resistance of low frequency arc; CPE2, constant phase element of low frequency arc.

that no deleterious interfacial reaction takes place between the 1Ce10ScZr grains and the YSZ electrolyte layer during the co-firing at 1400 °C. Though the doping cations in the two zirconia electrolytes might diffuse into each other at high temperature, the ionic conductivity of Y_2O_3–Sc_2O_3–ZrO_2 system is still much higher than that of the YSZ electrolyte [29,30]. Accordingly, the deleterious reaction, which often occurs between the doped ceria and the YSZ electrolyte film during co-firing [13,14], does not occur in our experiments.

Leng et al. proposed an equivalent circuit to quantitatively evaluate the EIS spectra [9], as illustrated in Fig. 4. Inductor L, at high frequency range, is originated from metal current collectors and leads. Resistance R_0, intercept on real axis at high frequency region, represents the total ohmic resistance. The arc (R_1, CPE1) at high frequency range reflects the charge transfer of oxide ions. And the semicircle (R_2, CPE2) at low frequency range is mostly influenced by the oxygen dissociative adsorption and/or surface diffusion of oxygen species at the LSM–YSZ surface. The impedances from H_2 electrochemical oxidation at anode and from YSZ grain boundary are neglected considering the small and unaltered impedance sizes of these processes. The EIS spectra were simulated by a complex non-linear least-square (CNLS) fitting program according to the equivalent circuit. The fitted parameters and their error% of the standard cell at 650 and 800 °C are taken as examples in Table 1. R_1, the charge transfer resistance, is given in Fig. 5 as a function of temperature. At 800 °C, R_1 decreases from 0.24 Ω cm^2 for the unmodified cell to 0.18 Ω cm^2 for the 1Ce10ScZr modified one. At 650 °C, R_1 significantly decreases from 0.82 to 0.38 Ω cm^2 after modification. So, the modification effec-

Table 1
Impedance parameters evaluated by CNLS program for the unmodified cell at 650 and 800 °C

Parameters	650 °C		800 °C	
	Value	Error%	Value	Error%
L (H)	1.1E−6	0.22	1.1E−6	0.47
R_0 (Ω cm^2)	0.21	0.32	0.11	2.3
R_1 (Ω cm^2)	0.34	2.1	0.23	3.8
CPE1-T	0.019	2.4	0.036	7.4
CPE1-P	0.43	1.1	0.47	1.5
R_2 (Ω cm^2)	0.82	0.86	0.24	3.6
CPE2-T	0.018	2.27	0.045	2.9
CPE2-P	0.33	0.40	0.22	1.6

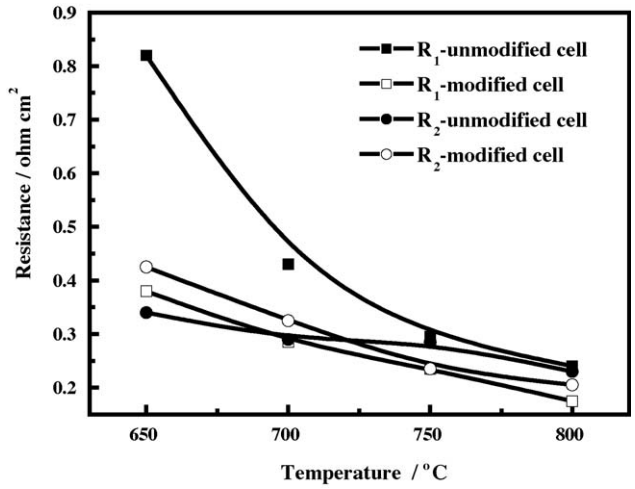

Fig. 5. Temperature dependence of R_1 and R_2 of the cells with and without the 1Ce10ScZr modification.

tively reduced the charge transfer resistance, especially at lower temperatures. R_2, the surface diffusion resistance is also shown in Fig. 5. No significant decrease of R_2 is observed after the 1Ce10ScZr modification at cathode/electrolyte interface.

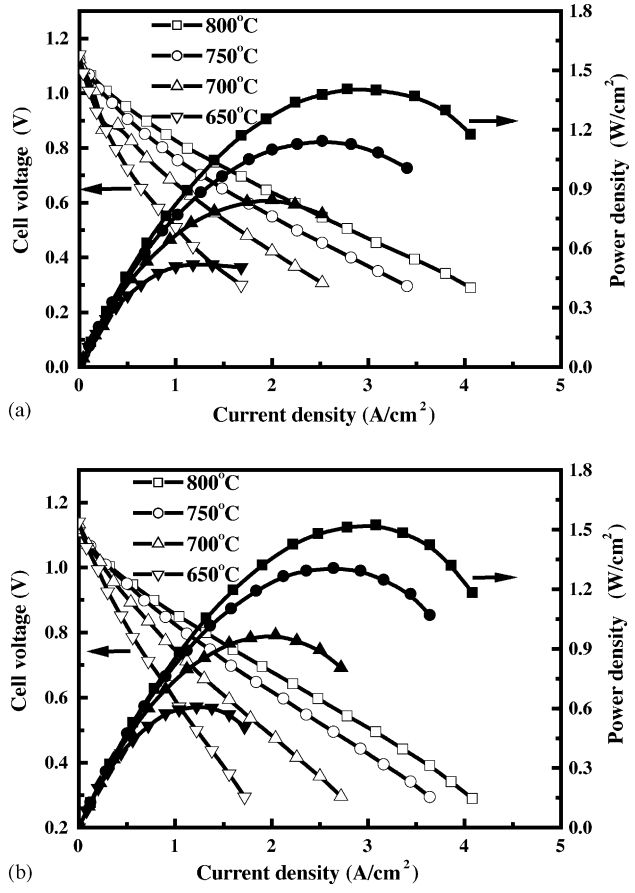

Fig. 6. Output performance of the single cells with and without the 1Ce10ScZr modification: (a) unmodified cell and (b) modified cell.

3.3. Cell performance

Fig. 6 displays the output performance of the cells with and without 1Ce10ScZr modification. The two cells display the similar open circuit voltage of about 1.12 V at 800 °C, nearly equal to the theoretical value. This indicates the good gas tightness of the YSZ electrolyte layer after the 1Ce10ScZr modification, which is consistent with the SEM observations in Fig. 2. At 800 °C, the modified cell gives a power density of 1.32 W cm^{-2} at 0.7 V and a maximum power density of 1.53 W cm^{-2}, and whereas the corresponding values are 1.17 and 1.41 W cm^{-2} for the unmodified cell. At 650 °C, the modified cell shows a power density of 0.53 W cm^{-2} at 0.7 V, which is 40% higher than the 0.38 W cm^{-2} for the unmodified one. The performance improvement is more significant at lower temperature, which is consistent with the decrease of charge transfer resistance after the modification.

4. Conclusions

The 1Ce10ScZr modification at the cathode/electrolyte interface reduced the charge transfer resistance of oxide ions from the LSM–YSZ composite cathode surface to the YSZ electrolyte surface, which was mainly attributed to the faster surface oxygen exchange rate of 1Ce10ScZr grains than the YSZ electrolyte film. The modification improved cell performance, especially at the lower temperatures. The 1Ce10ScZr modification at cathode/electrolyte interface provides a new, simple and cost-effective approach to improve the cell performance. At last, the modification is helpful to understand the electrochemical essence at electrode/electrode interface of SOFC.

Acknowledgements

The authors gratefully acknowledge financial supports from the Ministry of Science and Technology of China (Grant No. 2004CB719506) and the Chinese Academy of Sciences (Grant No. KGCX-X2-SW-311).

References

[1] B.C.H. Steel, A. Heinzel, Nature 414 (2001) 345.
[2] O. Yamamoto, Electrochim. Acta 45 (2000) 2423.
[3] R. Doshi, V.L. Richards, J.D. Carter, X. Wang, M. Krumpelt, J. Electrochem. Soc. 146 (1999) 1273.
[4] T. Ishihara, T. Shibayama, M. Honda, H. Nishiguchi, Y. Takita, Chem. Commun. (1999) 1227.
[5] K. Kobayashi, I. Takahashi, M. Shiono, M. Dokiya, Solid State Ionics 152–153 (2002) 591.
[6] S.D. Souza, S.J. Visco, L.C.D. Jonghe, J. Electrochem. Soc. 144 (1999) 35.
[7] S.P. Yoon, J. Han, S.W. Nam, T.H. Lim, I.H. Oh, S.A. Hong, Y.S. Yoo, H.C. Lim, J. Power Sources 106 (2002) 160.
[8] Y. Jiang, A.V. Virkar, J. Electrochem. Soc. 148 (2001) A706–A709.

[9] Y.L. Leng, S.H. Chan, K.A. Khor, S.P. Jiang, Int. J. Hydrogen Energy 29 (2004) 1025.
[10] Y. Jiang, A.V. Virkar, J. Electrochem. Soc. 150 (2003) A942.
[11] S.P. Simner, J.F. Bonnett, N.L. Canfield, K.D. Meinhardt, J.P. Shelton, V.L. Sprekle, J.W. Stevenson, J. Power Sources 113 (2003) 1.
[12] M. Shiono, K. Kobayashi, T.L. Nguyen, K. Hosoda, T. Kato, K. Ota, M. Dokiya, Solid State Ionics 170 (2004) 1.
[13] A. Tsoga, A. Gupta, A. Naoumidia, P. Nikolopoulos, Acta Mater. 48 (2000) 4709.
[14] H. Mitsuyasu, Y. Nonaka, K. Eguchi, Solid State Ionics 113–115 (1998) 279.
[15] M. de Ridder, A.G.J. Vervoort, R.G. Van Welzenis, H.H. Brongersma, Solid State Ionics 156 (2003) 255.
[16] M. Kuznecov, P. Otschik, P. Obenaus, K. Eichler, W. Schaffrath, Solid State Ionics 157 (2003) 371.
[17] E.P. Murry, T. Tsai, S.A. Barnett, Solid State Ionics 110 (1998) 235.
[18] Y.K. Lee, J.Y. Kim, Y.Ki. Lee, I. Kim, H.S. Moon, J.W. Park, C.P. Jacobson, S.J. Visco, J. Power Sources 115 (2003) 219.
[19] S.P. Jiang, J. Power Sources 124 (2003) 390.
[20] T. Tsai, S.A. Barnett, Solid State Ionics 98 (1997) 191.
[21] T. Tsai, S.A. Barnett, J. Electrochem. Soc. 145 (1998) 1696.
[22] E.P. Murray, T. Tsai, S.A. Barnett, Nature 12 (1999) 649.
[23] D. Herbstritt, A. Weber, E. Iivers-Tiffée, J. Eur. Ceram. Soc. 21 (2001) 1813.
[24] A. Weber, E.I. Tiffée, J. Power Sources 127 (2004) 273.
[25] H. Uchida, M. Yoshida, M. Watanabe, J. Electrochem. Soc. 146 (1999) 1.
[26] D.S. Lee, W.S. Kim, S.H. Choi, J. Kim, H.W. Lee, J.H. Lee, Solid State Ionics 176 (2005) 33–39.
[27] Z.W. Wang, M.J. Cheng, Z.H. Bi, Y.L. Dong, H.M. Zhang, J. Zhang, Z.C. Feng, C. Li, Matter. Lett. 59 (2005) 2579–2582.
[28] B.C.H. Steel, K.M. Hori, S. Uchino, Solid State Ionics 135 (2000) 445.
[29] S.P.S. Badawal, F.T. Ciacchi, S. Rajendran, J. Drennan, Solid State Ionics 109 (1998) 167.
[30] T.I. Politave, J.T.S. Irvine, Solid State Ionics 168 (2004) 153–165.